

# Extraction of microalgal starch and pigments by using different cell disruption methods and aqueous two-phase system

Fabrizio Di Caprio,<sup>\*</sup>  Rachele Chelucci, Iolanda Francolini, Pietro Altimari and Francesca Pagnanelli



## Abstract

**BACKGROUND:** Microalgae can synthesize starch with productivity higher than conventional terrestrial crops, without the need for arable land. However, little is known about processes to extract starch from microalgae. Here, a biorefinery process is described including microalgal cell disruption followed by extraction of starch and pigments with aqueous two-phase system (ATPS) using choline chloride and polypropylene glycol 400. Sonication and bead milling were compared for cell disruption rate and starch extraction efficiency.

**RESULTS:** A first order kinetic model described well the cell disruption for both the methods, with a rate 2.6 times higher for bead milling than sonication. By applying ATPS on samples with comparable cell disruption (>93%), starch was separated better after sonication (67% recovery in the pellet) than after bead milling, for which it remained equally distributed between pellet (40%) and choline chloride phase. Pigments were extracted with 42–66% yield irrespective of the cell disruption method. Microalgal starch granules had a normal and narrow distribution for size ( $0.93 \pm 0.14 \mu\text{m}$ ) and a gelatinization temperature between 45–55 °C.

**CONCLUSION:** For the same cell disruption yield, different starch separation efficiencies can be achieved, depending on the cell disruption method applied. Although bead milling was faster than sonication in disrupting cells, it gave worst starch separation efficiency. The properties of the extracted microalgal starch indicate potential technical advantages, with respect to conventional starch sources, for applications in the bioplastic and food sector.

© 2021 The Authors. *Journal of Chemical Technology and Biotechnology* published by John Wiley & Sons Ltd on behalf of Society of Chemical Industry (SCI).

Supporting information may be found in the online version of this article.

**Keywords:** *Tetrademus obliquus*; aqueous two-phase system; bioplastic; wet extraction; biorefinery; energy cost

## INTRODUCTION

Microalgae are a promising future new source of starch because they are potentially able to attain starch productivities ( $\text{t ha}^{-1} \text{y}^{-1}$ ) up to ten folds higher than conventional terrestrial plants, such as corn.<sup>1</sup> In addition, contrarily to conventional terrestrial crops, microalgae can be cultivated on wastewaters, saltwater, and non-arable lands. When cultivated under specifically tailored conditions (e.g. nitrogen starvation), microalgae can accumulate remarkable starch content, up to 40–45% of dry weight.<sup>1–4</sup> Microalgal starch could be potentially used for several industrial applications, such as bioplastics,<sup>5</sup> food ingredients and carrier materials.<sup>6</sup> However, to date, there is little information about the properties of microalgal starch. Microalgal starch contains granules between 0.5–1.5  $\mu\text{m}$ , with 17–29% amylose.<sup>1,7</sup> No relevant information was found about its gelatinization temperature and granule size distribution, which are very important parameters to know for developing appropriate extraction processes and for practical applications. A major limitation in studying and using

microalgal starch is given by the difficulties encountered for its extraction and purification. Since starch is insoluble in solvents in its native form, the general approach for starch extraction considers two main steps: (i) cell disruption to allow the release of the intracellular starch granules, without relevant starch degradation; (ii) starch purification by its separation from the other biomolecules, usually performed by starch precipitation. However, the conventional procedures used to extract starch from terrestrial plant sources are ineffective with microalgae, likely because microalgal cells have size (~2–10  $\mu\text{m}$ ) lower than terrestrial plant cells (~10–100  $\mu\text{m}$ ), lower size of starch granules, lower starch content (40–45%) than the plant cells inside the grains (~75%),

<sup>\*</sup> Correspondence to: F Di Caprio, Dipartimento di Chimica, Sapienza Università di Roma, Piazzale Aldo Moro 5, 00185, Rome, Italy. E-mail: fabrizio.dicaprio@uniroma1.it

Dipartimento di Chimica, Sapienza Università di Roma, Rome, Italy

and microalgal cell walls are hard to break down for the presence of resistant polymers such as sporopollenin.<sup>8</sup>

Different cell disruption methods were applied to obtain microalgal starch, including sonication,<sup>9</sup> bead milling,<sup>1,10,11</sup> and French pressing.<sup>12</sup> However, in these studies the starch recovery yield was not assessed, the different cell disruption methods were not compared, and the starch was purified through centrifugation on Percoll<sup>®</sup> gradient, that is hardly scalable to process volumes larger than a few milliliters. Different cell disruption methods have been compared mainly for the extraction of proteins and lipids, while little is known about the effects of these methods on starch extraction. Furthermore, the comparisons were usually performed without ensuring that the same cell disruption yield was attained by the different cell disruption methods. With this approach, the differences found on the extraction yield attained with different cell disruption methods might have been simply related to the achievement of different cell disruption yields. A recent review underlined how this approach is hampering the comparison of results reported in previous studies.<sup>13</sup> The authors suggested to use cell counting as an objective way to assess cell disruption efficiency. In accordance with this principle, an objective comparison of the effects of different cell disruption methods on biomolecule extraction efficiency should be performed by evaluating the extraction yields attained on samples delivered by the different disruption methods at identical cell disruption yield.

Recently, aqueous two-phase systems (ATPS) were reported as promising scalable method to separate microalgal starch from other cellular components (proteins, soluble sugars, and pigments) after cell disruption. In this framework, the protocol developed by Suarez Ruiz and co-workers was based on the utilization of polypropylene glycol 400 (PPG 400), choline dihydrogen phosphate and water.<sup>10,11</sup> By applying this method after cell disruption by bead milling, 79% of starch was recovered from *Neochloris oleoabundans* at the interface, while 82% proteins were separated in the bottom phase (water - choline dihydrogen phosphate) and 98% pigments in the upper phase (water- PPG 400).<sup>11</sup>

Based on this literature survey, three major gaps were identified: (i) the effect of different cell disruption methods on starch recovery is not known. (ii) The ATPS previously used included only the utilization of choline dihydrogen phosphate, that is currently an expensive and hardly obtainable chemical for larger industrial volumes. (iii) Little is known about the properties of microalgal starch, such as gelatinization temperature and granule size distribution.

Therefore, the aim of this work was to fill in these gaps. To this end, two of the most promising cell disruption methods for large scale application (sonication and bead milling), were compared for their effects on starch and pigment extraction yield and repartition among the different ATPS phases. The ATPS used in this study was made with choline chloride, which is a chemical cheaper and more available than the previously tested choline dihydrogen phosphate. The comparison was performed by using cell lysates produced by the two different methods with the same cell disruption yield. The obtained starch was finally characterized in terms of granule size distribution and gelatinization temperature.

## MATERIAL AND METHODS

### Microalgae cultivation

A strain of the microalga *Tetrademus obliquus* (generally known as *Scenedesmus obliquus*) was selected and identified as

previously described.<sup>14</sup> The strain was maintained in solid and liquid BG11 medium, in phototrophic and non-axenic conditions, as previously described.<sup>14</sup> Microalgae suspension was then transferred to two 500 mL column photobioreactors (h = 35 cm, d = 5 cm) made of glass, attaining an initial biomass concentration of 0.1 g L<sup>-1</sup>. The reactors were filled with the following culture medium: KNO<sub>3</sub> 10 mM; Na<sub>2</sub>SO<sub>4</sub> 0.7 mM; MgSO<sub>4</sub>·7H<sub>2</sub>O 1 mM; CaCl<sub>2</sub>·2H<sub>2</sub>O 0.5 mM; K<sub>2</sub>HPO<sub>4</sub> 2.5 mM; NaHCO<sub>3</sub> 10 mM; NaFeEDTA 28 μM; Na<sub>2</sub>EDTA·2H<sub>2</sub>O 80 μM; MnCl<sub>2</sub>·4H<sub>2</sub>O 19 μM; ZnSO<sub>4</sub>·7H<sub>2</sub>O 4 μM; CoCl<sub>2</sub>·6H<sub>2</sub>O 1.2 μM; CuSO<sub>4</sub>·5H<sub>2</sub>O 1.3 μM; Na<sub>2</sub>MoO<sub>4</sub>·2H<sub>2</sub>O 0.1 μM. The culture medium was filtered through 0.7 μm filters before use. The temperature of the culture was maintained at 28 ± 1 °C and the pH at 7.5 ± 0.5. The photobioreactors were illuminated 24 h with 35 W led light lamps (equally composed by 6500 K and 4000 K strips) supplying 200 μmol s<sup>-1</sup> m<sup>-2</sup> photons. The reactors were continuously fed with 1 L min<sup>-1</sup> air (filtered by 0.2 μm filter) and 10 mL min<sup>-1</sup> pure CO<sub>2</sub>. The cultivation was repeated in three sequential batches under the same conditions, and each batch was replicated in two separate column photobioreactors. The biomass concentration was monitored by measuring the dry weight during the cultivation. When a concentration of 3.0–3.5 g L<sup>-1</sup> was attained, the batch was stopped and the biomass was harvested by centrifugation at 3000 × g, rinsed twice with distilled water and suspended in distilled water at 90 g L<sup>-1</sup> and frozen at -18 °C until its utilization for cell disruption treatment. Dry weight was measured by filtering the samples through 0.7 μm glass fiber filters, then dried at 105 °C. The aliquots of biomass harvested from three independent cultivations carried out in the same culture conditions were used as replicates for the following experiments.

### Cell disruption methods

#### Sonication

The microalgal suspension (20 mL, 90 g L<sup>-1</sup>) was defrosted and then treated with sonication. The suspension was transferred to a 50 mL glass reactor (h = 5 cm, d = 4.4 cm) with an external jacket connected to a thermocryostat (CB5-10, Giorgio Bormac srl, Modena, Italy) for cooling water recirculation. The recirculation water was maintained at 6 °C to maintain the microalgal suspension below 35 °C throughout the treatment. The sonication was started when the microalgal suspension was at 6 °C by using the Branson 450 Digital Sonifier (20 kHz, 400 W maximum output power) at 60% amplitude (90 μm) and in pulsed mode with t<sub>on</sub>/t<sub>off</sub> = 0.3/0.1 s, t<sub>on</sub> and t<sub>off</sub> denoting the time interval during which the supply of mechanical energy was active and inactive, respectively. A 12 mm replaceable horn probe was used for the sonication and immersed inside the suspension. Cell concentration was measured throughout the treatment by optical counting in a Thoma chamber by means of an optical microscope (Leitz Laborlux 12). The experiment was carried out in triplicate.

#### Bead milling

The microalgal suspension (1 mL, 90 g L<sup>-1</sup>) was defrosted and then treated with the bead beater (Minily, Bertin Technologies, Montigny-le-Bretonneux, France). Microalgal samples were placed inside 2 mL beating tubes containing 0.1 mm ZrO<sub>2</sub> beads (Precellys - Ref: KT03961-1-010.2). Samples were treated with several (up to 25) milling cycles, 60 s each one (t<sub>on</sub>), at 5000 rpm. Between cycles the tubes were placed for 120 s (t<sub>off</sub>) on ice batch for cooling. The temperature was measured at each cycle before and after the cooling. Cell concentration was measured after each cycle by optical counting.

### Analysis of cell disruption kinetics

With both the sonication and bead milling, the cell disruption yield was determined by Eqn (1):

$$\text{Cell disruption } (T_{on})(\%) = \frac{C_{cells,0} - C_{cells}(T_{on})}{C_{cells,0}} 100 \quad (1)$$

With  $C_{cells,0}$  and  $C_{cells}(T_{on})$  denoting the initial cell concentration and the concentration measured at a treatment time  $T_{on}$ . The time  $T_{on}$  appearing in Eqn (1) is the sum of the  $t_{on}$  times elapsed since the start of the cell disruption treatment ( $T_{on} = \sum_{t=0}^t t_{on}$ ). The  $t_{off}$  was not included in the kinetic study because it was assumed that the cell disruption yield was only depending on the sum of the elapsed  $t_{on}$  periods, which was the period in which the mechanical energy was applied. The  $t_{off}$  was set up mainly to avoid overheating of the biomass suspension. It would not be consistent to compare sonication and bead milling based on the sum of the  $t_{on}$  and  $t_{off}$  periods, because much larger  $t_{off}$  times were necessary in the application of bead milling method just to control the temperature. This different  $t_{off}$  period could be removed at industrial scale by the utilization of a cooling water jacket. The kinetics of cell disruption were analyzed by fitting the solution of the following first order model (Eqn (2)) to the evolution of cell disruption data against  $T_{on}$ :

$$\frac{dC_{cells}}{dT_{on}} = -kC_{cells}(T_{on}) \quad (2)$$

The kinetic constant  $k$  was estimated by nonlinear fitting of the experimental data to the Eqn (3):

$$C_{cells}(T_{on}) = C_{cells,0} e^{-kT_{on}} \quad (3)$$

where  $C_{cells,0}$  denotes the initial cell concentration.

### Extraction with aqueous two-phase system (ATPS)

After cell disruption, the obtained lysed biomass suspensions were treated with ATPS for biomolecule separation. ATPS was composed by polypropylene glycol- 400 (PPG-400; AlfaAesar, Ref. 40811) and choline chloride (98%, Alfa Aesar, Ref. A15828) with 40:14 w/w ratio, as described in a previous work.<sup>11</sup> For the preparation of the ATPS, 3.6 g of distilled H<sub>2</sub>O, 1.4 g di choline chloride, 4.0 g di PPG-400 and 1 mL (1 g) of lysed microalgal suspension obtained from sonication or bead milling (containing 90 mg biomass equivalent) were mixed in 15 mL polypropylene centrifuge tubes (VWR International, Ref. 525-0629). The components were mixed in the dark for 1 h in a rotary shaker at 25 rpm at room temperature, according to the method reported by Suarez Ruiz and co-workers.<sup>11</sup> After that, samples were centrifuged at 1670 × *g* for 10 min to favor phase separation and the upper (PPG 400) and bottom phase (ChCl) were separated with a glass pipette. The interface and pellet were submitted to a second and a third extraction cycle. All the obtained solid and liquid phases were separated and stored at -18 °C in the dark. The experiment was carried out in triplicate, each replicate corresponding to the lysate biomass obtained by repeated cell disruption treatments.

### Starch quantitative analysis

Starch was analyzed in initial microalgal biomass before cell disruption and on the pellet phase, interphase and bottom liquid

phase obtained after the ATPS extraction. For the analysis, the mass of starch was quantified by means of selective enzymatic hydrolysis by using the thermostable α-amylase and amyloglucosidase from the commercial Total Starch assay kit (Megazyme, ref. K-TSTA, Ireland), following the protocol as described by de Jaeger *et al.*<sup>15</sup> The recovery yield of starch in the different phases ( $\eta_{starch,i}$ ) was calculated by Eq. 4:

$$\eta_{starch,i} = \frac{V_i C_{S,i}}{m_X C_{S,X}} \quad (4)$$

with  $V_i$  the volume of the  $i$ -phase (interphase, pellet phase, bottom phase),  $C_{S,i}$  the starch concentration in the  $i$ -phase,  $m_X$  the initial biomass used for ATPS extraction and  $C_{S,X}$  the starch content in this biomass (measured before cell disruption).

### Scanning electron microscope (SEM) and granule size measurement

For SEM analysis, the samples were pretreated for fixation and dehydration. An aliquot of sample (0.1 mL) was centrifuged at 3000 × *g* for 10 min and supernatant was removed. The pellet was suspended in 1 mL of PBS (Phosphate Buffer Saline) solution at 2% of glutaraldehyde and stored in the fridge for 1 h. The sample was centrifuged again, and the supernatant was removed. The pellet was then suspended in ethanol-water solution with increasing ethanol content: 30%, 50%, 70%, 80%, 90% and 100%. A drop of the suspension in ethanol was placed on a microscope glass slide and quickly evaporated. Samples were covered with a thin chromium film and finally analyzed by means of a HR-FESEM (High resolution Field Emission Scanning Electron Microscopy) model AURIGA Zeiss. Starting from the obtained micrographs, the diameter of 100 starch granules was determined using ImageJ software. The distribution of starch granule size was modelled by Gaussian distribution (Eqn (5)):

$$f(x) = \frac{1}{\sigma\sqrt{2\pi}} e^{-\frac{(x-\mu)^2}{2\sigma^2}} \quad (5)$$

With  $x$  the diameter,  $\mu$  the mean diameter and  $\sigma$  the standard deviation of the diameter.

### Determination of starch gelatinization temperature

This analysis was conducted on starch in the pellet phase obtained after ATPS extraction on sonicated biomass. The pellet phase was placed on a microscope slide and covered with glass cover slide. The sample was placed on a block heater and gradually heated at different temperatures (Supporting Information, Fig. S1). To account for the temperature gradient along the glass slide, the temperature was measured both at the bottom and upper side of the slide. Different temperature ranges were assessed: 25 °C, 30–35 °C, 45–50 °C and 50–55 °C. The sample was maintained 30 min on the preheated block for each different temperature range and then observed on the optical microscope (Leitz Laborlux 12) to detect whereas starch gelatinization occurred.

### Determination of pigment extraction yield

The extraction yield of photosynthetic pigments was determined on the upper phase (PPG-400) by spectrophotometric analysis (Varian Cary 50 Scan). The content of Chlorophyll a, Chlorophyll b and carotenoids inside the initial biomass was determined as follows. Microalgal biomass was centrifuged (8000 × *g*, 10 min)

and the aqueous supernatant was removed. The pellet was suspended in acetone and heated for 30 min at 50 °C. Acetone was then collected and the absorbance was measured at 661.6 nm, 644.8 nm and 470 nm. From the absorbance values, the pigment concentration was quantified by using the equations reported by Lichtenthaler.<sup>16</sup> To quantify the pigments extracted with PPG-400, a correlation line was made between pigment absorbance in PPG-400 and their absorbance in acetone. To this aim, pigments were extracted with acetone from different samples of microalgae and analyzed as described. After analysis, acetone was evaporated under N<sub>2</sub> flow and the residual pigments were suspended in equal volume of PPG-400 and analyzed with the spectrophotometer, using the same wavelengths as for acetone. The correlation lines (Eqns (6)–(8)) were determined and applied to obtain the equivalent absorbance in acetone.

$$OD_{661.6,PPG-400} = 0.80 OD_{661.6,Acetone} \quad R^2 = 0.99 \quad (6)$$

$$OD_{644.8,PPG-400} = 0.85 OD_{644.8,Acetone} \quad R^2 = 0.97 \quad (7)$$

$$OD_{470,PPG-400} = 0.56 OD_{470,Acetone} \quad R^2 = 0.98 \quad (8)$$

For each upper phase (in PPG-400) obtained in the samples after the three ATPS cycles, the absorbance was read directly in PPG-400, the corresponding absorbance in acetone was calculated and used to quantify pigment concentration.

The pigment recovery yield was calculated by Eqn (9).

$$\eta_p = \frac{V_{PPG} C_{p,PPG}}{m_X C_{p,X}} \quad (9)$$

With  $V_{PPG}$  the volume of the PPG 400 phase,  $C_{p,PPG}$  the concentration of pigment in the PPG400 phase and  $C_{p,X}$  the concentration of pigment inside the initial biomass (measured before cell disruption).

### Statistical treatment of data

All the experiments were carried out in triplicate and the results reported as mean  $\pm$  standard error (SE). Significant differences ( $\alpha = 0.05$ ) among treatments were evaluated by using one way analysis of variance (ANOVA) or Student's *t*-test. Nonlinear fitting was performed by the MATLAB function 'nlinfit', which performs the minimization of the sum of the squared residuals. The uncertainty in model parameter prediction was indicated with 95% confidence intervals (CI), calculated with the MATLAB function 'nlparci'.

## RESULTS AND DISCUSSION

### Biomass and starch production by microalgae

Microalgae were cultivated in photobioreactors under their optimal growth conditions (pH = 7.5, T = 28 °C, nutrient replete).<sup>17</sup> The biomass increased from 0.1 g L<sup>-1</sup> to 3.2  $\pm$  0.2 g L<sup>-1</sup> in 4 days (Fig. 1(A)), corresponding to an average biomass productivity of 0.78  $\pm$  0.05 g L<sup>-1</sup> per day. This growth corresponded to the biological CO<sub>2</sub> fixation of 1.43  $\pm$  0.09 g L<sup>-1</sup> per day (about 6% of the supplied CO<sub>2</sub>). The nitrogen source (NO<sub>3</sub><sup>-</sup>) was depleted after 2 days of cultivation (Fig. 1(B)). With the aim to increase the biomass starch content, the cultivation was prolonged for 2 days under nitrogen (N) starvation condition. During N-starvation, cell duplication was blocked (because of the exit from the cell cycle, G<sub>0</sub>) and the biomass increase was mainly given by the accumulation of storage compounds, including starch. The starch content

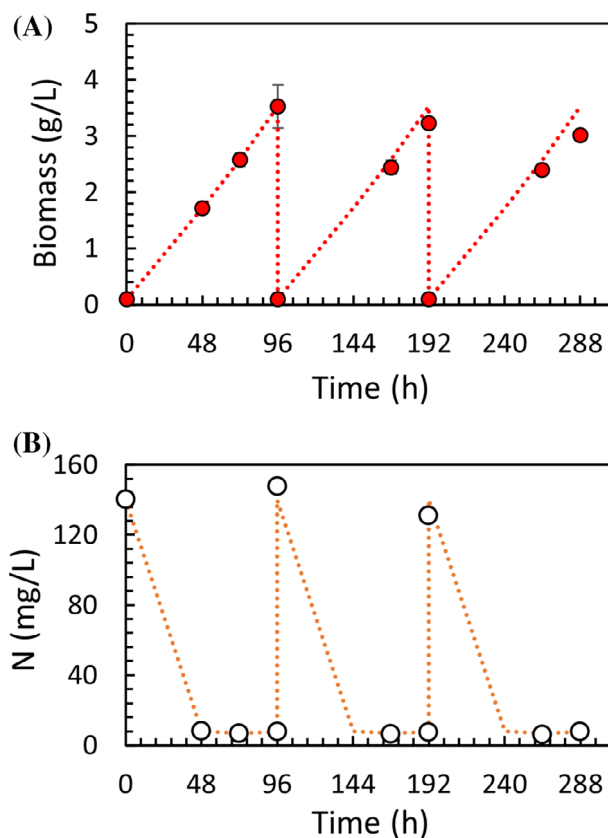


**Figure 1.** Biomass production (A) and nitrogen consumption (B) on three repeated batches. Mean value  $\pm$  SE,  $n = 2$ . Dotted lines indicate the repetition of the points of the first batch, to show the reproducibility of the growth.

attained in the biomass harvested at the end of the batches was 33%  $\pm$  4%, significantly higher ( $P = 3 \times 10^{-6}$ ) than the starch content in the first two cultivation days (N-replete), which was only 9.6%  $\pm$  1.5%. These results are comparable with those reported by Breuer *et al.*,<sup>3</sup> who found, for the same species and with the same cultivation medium, 38% starch content when a biomass concentration of 3.1 g L<sup>-1</sup> was attained. The starch content attained is slightly lower than the maximum value reported for this species, which is 42%.<sup>18</sup> The mean starch productivity of the batches was 0.25  $\pm$  0.02 g L<sup>-1</sup> per day. The biomass harvested at the end of the batch contained 4.4%  $\pm$  0.6% of N, corresponding to 28%  $\pm$  4% proteins, significantly lower ( $P = 0.006$ ) than the protein content attained in the first 2 days under N-replete conditions (54%  $\pm$  1%).

### Comparison between sonication and bead milling on cell disruption efficiency

The biomass enriched in starch was harvested from the photobioreactors and employed to evaluate the ability of the selected cell disruption treatments to enforce the release of intracellular starch granules.

Native starch is made of insoluble molecules (amylose and amylopectin) of high molecular weight (typically >40 000 Da), which are partially in crystalline form and arranged in granules inside the chloroplasts. Starch granules are typically insoluble in solvents. Therefore, the extraction of starch from cells requires cell disruption to allow the release of the insoluble granules and their subsequent separation from the other biomolecules. Chemical

methods based on acids or alkaline reagents cannot be applied for cell disruption because they would induce starch hydrolysis and/or gelatinization. Therefore, two different physical methods were tested, namely sonication and bead milling, which are among the most promising for large scale application. The treatments were applied on a biomass suspension with relatively high biomass concentration ( $90 \text{ g L}^{-1}$ ), which can be considered representative of a suspension obtained in a real plant after a dewatering phase (harvesting). The two methods were separately applied until reaching comparable ( $P > 0.05$ ) cell disruption yields, which was  $93\% \pm 3\%$  for bead milling and  $97\% \pm 1\%$  for sonication. The evolution of cell concentration during both bead milling and sonication was satisfactorily described by the first order kinetic model (Eqn (3)) (Fig. 2), which is in agreement with other previous studies.<sup>19,20</sup> In Fig. 2, a comparison between experimental data (cell disruption yield and cell concentration) and the predictions of the first order model with the kinetic constant  $k$  determined by nonlinear fitting is shown for the two cell disruption methods. It is important to notice that cell disruption yield and cell concentration are plotted in Fig. 2 against the  $T_{\text{on}}$ , which is the sum of the  $t_{\text{on}}$  periods and thus represents the time during which mechanical energy was effectively supplied to the system, excluding the  $t_{\text{off}}$  periods. In accordance with this analysis, the characteristic time needed with bead milling to attain the prescribed cell disruption yield was about 2.6 times lower than with sonication. Particularly, the kinetic constant  $k$  estimated by nonlinear fitting of Eqn (3) to the evolution of cell concentration data against  $T_{\text{on}}$  was  $0.063 \pm 0.008 \text{ min}^{-1}$  with bead milling and  $0.024 \pm 0.002 \text{ min}^{-1}$  with sonication ( $P < 0.05$ ), corresponding to characteristic times ( $\tau = k^{-1}$ ) of 16 min and 42 min, respectively. The  $k$  found for bead milling was remarkably lower than those found in previous studies,<sup>20,21</sup> which were between  $0.54 \text{ min}^{-1}$  and  $4.8 \text{ min}^{-1}$ . This difference could be explained by differences in the specifications of the employed bead milling system, including, for example, bead size, filling percentage and the microalgal strain tested.<sup>20,21</sup> In this respect, it is worth

remarking that the microalga *T. obliquus* employed in the present study is one of the microalgal species with higher cell wall robustness,<sup>22-24</sup> and it was not considered in the previous studies using bead milling.

The temperature was controlled and monitored during the treatments to avoid any starch denaturation due to temperature increase. It was maintained at comparable values for the two methods (Supporting Information, Fig. S2). During sonication it increased rapidly (within less than 5 min) from  $6 \text{ }^\circ\text{C}$  up to  $27 \pm 5 \text{ }^\circ\text{C}$ , and then remained stable throughout the treatment. During bead milling, the temperature oscillated by increasing during the milling phase ( $t_{\text{on}}$ ) to  $32 \pm 1 \text{ }^\circ\text{C}$  and then decreasing during the cooling phase ( $t_{\text{off}}$ ) to  $21 \pm 1 \text{ }^\circ\text{C}$  (the mean value of the whole treatment was  $27 \text{ }^\circ\text{C}$ ).

Few data are available from previous studies about the comparison between the effects of sonication and other different methods on microalgal cell disruption yield. A previous study indicated, in agreement with our results, that sonication was less effective than bead milling.<sup>25</sup> Other studies indicated that sonication was less effective also when compared to other methods, such as high-pressure homogenization.<sup>13,26</sup> However, the comparison was often performed based on data derived by the application of the different cell disruption treatments with different treatment times and temperatures. Therefore, the results reported here in this study are a more solid comparison and indication about the better performance of bead milling. In this study, the two treatments were compared by considering only the time during which mechanical energy was effectively supplied to the system ( $T_{\text{on}}$ ), thus not including the off times ( $t_{\text{off}}$ ), which were  $0.33 \cdot t_{\text{on}}$  and  $2 \cdot t_{\text{on}}$  for sonication and bead milling, respectively (Fig. 2). Although the higher off time fraction for bead milling affects the difference in the time effectively required for the treatment, it is expected that this difference will be remarkably reduced at industrial scale, where a cooling jacket can be used for bead milling cooling, thus allowing for continuous milling.<sup>20</sup>

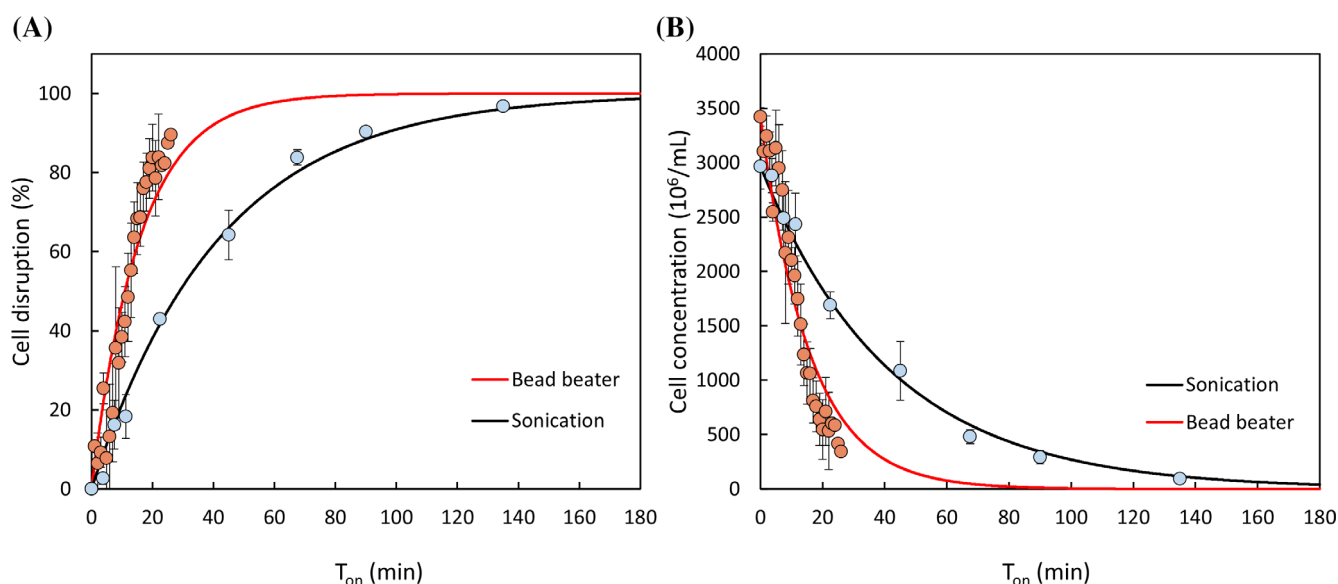


**Figure 2.** (A) Cell disruption yield (%) during bead beater and sonication treatment. (B) cell concentration during bead beater and sonication treatment. As treatment time, the  $t_{\text{on}}$  time was only considered, corresponding to the time of mechanical energy application ( $T_{\text{on}} = \sum_{t=0}^t t_{\text{on}}$ ). Circles indicate experimental data (mean value  $\pm$  SE,  $n = 3$ ) while lines indicate the fitting obtained with the first order kinetic model. The treatments were performed at  $90 \text{ g L}^{-1}$  biomass.

### Separation of starch with ATPS

The lysate biomass obtained from bead milling and sonication treatment was then processed for biomolecule separation by ATPS. ATPS made of PPG400-choline dihydrogen phosphate (ChDHp) aqueous phases was reported in previous studies to allow for the separation of pigments, proteins and starch from *N. oleoabundans* biomass previously lysed by bead milling.<sup>10,11,27</sup> In these latter studies, up to 79% of starch was recovered in the interphase after 3 cycles of extraction, while proteins and pigments were separated in the ChDHp and PPG400 phase respectively. In the present study, a similar system was employed to separate the different microalgal biomolecules starting from the two lysates obtained by sonication and bead milling. Although Suarez Ruiz *et al.* selected ChDHp as optimal bottom phase for ATPS,<sup>11</sup> we did not use ChDHp because it is quite expensive and its supply is difficult (to our knowledge, to date it is sold in Europe only by lolitec, Germany), making difficult its industrial use. Choline chloride (ChCl) showed better results in protein separation as compared to ChDHp,<sup>11</sup> and it is already produced at low cost in large amount at industrial scale, so it can be easily supplied sustaining the industrial scale-up of the proposed separation method. Therefore, it was studied in this study because of its better potential for large scale application.

After ATPS separation, four phases were obtained, namely an upper PPG-400-water phase, a solid interphase, a bottom ChCl-water phase and a solid pellet (Supporting Information, Fig. S3). This qualitative repartition was found with both the lysed biomasses from bead milling and sonication. The only difference was the presence of ZrO<sub>2</sub> beads in the pellet phase in case of application of the biomass produced by bead milling. These beads were not removed to minimize biomass loss, based on the assumption that they did not affect the repartition of the biomolecules in the ATPS.

The analysis of starch repartition indicated relevant differences ( $P < 0.01$ ) between the samples from bead milling and sonication (Fig. 3). Although a comparable cell disruption yield was achieved with the two methods, the starch repartition was better with the lysate biomass obtained by sonication. For this latter lysate biomass, the starch was preferentially recovered in the solid pellet phase with  $67\% \pm 7\%$  yield, and only  $14\% \pm 2\%$  in the interphase (Fig. 3). This repartition is qualitatively comparable to that observed for corn starch with PPG400-ChDHp, for which starch was preferably recovered in the bottom pellet.<sup>10</sup> We tested the PPG400-ChCl system also with pure corn starch and this was entirely recovered in the pellet phase, similarly to the *T. obliquus* starch. This behavior was expected considering that native starch is insoluble in water and its density ( $1.5 \text{ g mL}^{-1}$ ) is higher than PPG400 ( $1.01 \text{ g mL}^{-1}$ ) and water-ChCl ( $1.02 \text{ g mL}^{-1}$ ) phase.<sup>28</sup> When the lysate biomass from bead milling was used, the amount of starch that moved in the solid phases (pellet and interphase) was lower ( $P < 0.01$ ) than for biomass pre-treated with sonication (Fig. 3). When ATPS was performed after bead milling, starch did not accumulate preferentially in the pellet phase, rather it was equally distributed with  $\sim 40\%$  yield both in the pellet and water-ChCl bottom phase (Fig. 3). This means that for the biomass pre-treated with bead milling, a larger amount of starch remained suspended in the ChCl phase. The sum of starch mass inside the three phases gave 90% total yield for sonication treatment and 80% for bead milling, without significant difference. The missing 10–20% starch was likely lost in the laboratory procedures carried

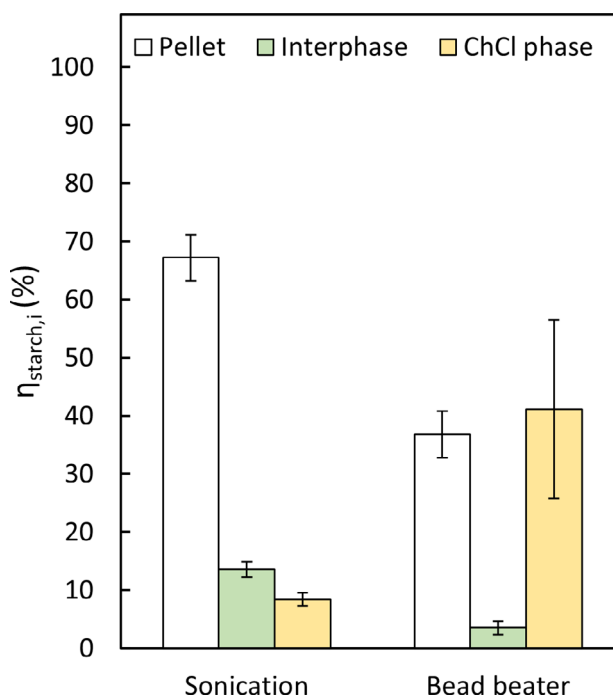


**Figure 3.** Recovery yield of starch ( $\eta_{\text{starch},i}$ ) obtained in three i-phases (pellet, interphase and ChCl phase) by ATPS performed on lysed biomass obtained after bead beater and sonication. Mean value  $\pm$  SE,  $n = 3$ .

out. It might be thought that the separation and recovery of starch should be mainly proportional to the cell disruption yield (namely, the release of starch granules outside cells). However, the results reported in this study indicated that the separation of microalgal starch is more complex. For our knowledge, this work is the first one in which such a remarkable difference in extraction yield is observed on samples with the same cell disruption yield, for microalgal starch. The reason for such a different behavior induced by the two cell disruption treatments may be explained by the different molecular interactions between starch and other biomolecules in the lysed biomasses obtained with the two methods. By looking at the SEM images (Fig. 4(B)–(E)), in the lysate obtained from sonication, the starch granules looked intact and well separated from the surrounding biomass, while, in the lysate from bead milling, the granules appeared partially degraded and more bridled inside the surrounding biomass. Therefore, it is possible that, after the bead milling treatment, there was a higher fraction of starch trapped inside cell fragments or still bound to hydrophilic compounds (e.g., proteins), or starch could partially degrade as result of milling. Such degraded starch could be more soluble, which can explain why a higher fraction of it remained in the aqueous ChCl phase. Yet, the two disruption treatments took different operative times to attain the same cell disruption yield. The sonication took  $\sim 2$  h, while bead milling took  $\sim 0.5$  h. These different times could give different yields in the separation of other intracellular biomolecules (e.g. proteins),<sup>21</sup> which could ultimately make the starch differently bound, affecting its repartition among the different phases.

For both the treatments, the fraction of starch in the interphase was the lowest (Fig. 3). This result is different to that by Suarez Ruiz *et al.*, who found starch preferentially recovered in the interphase.<sup>10,11</sup> This difference may be explained by the use in the

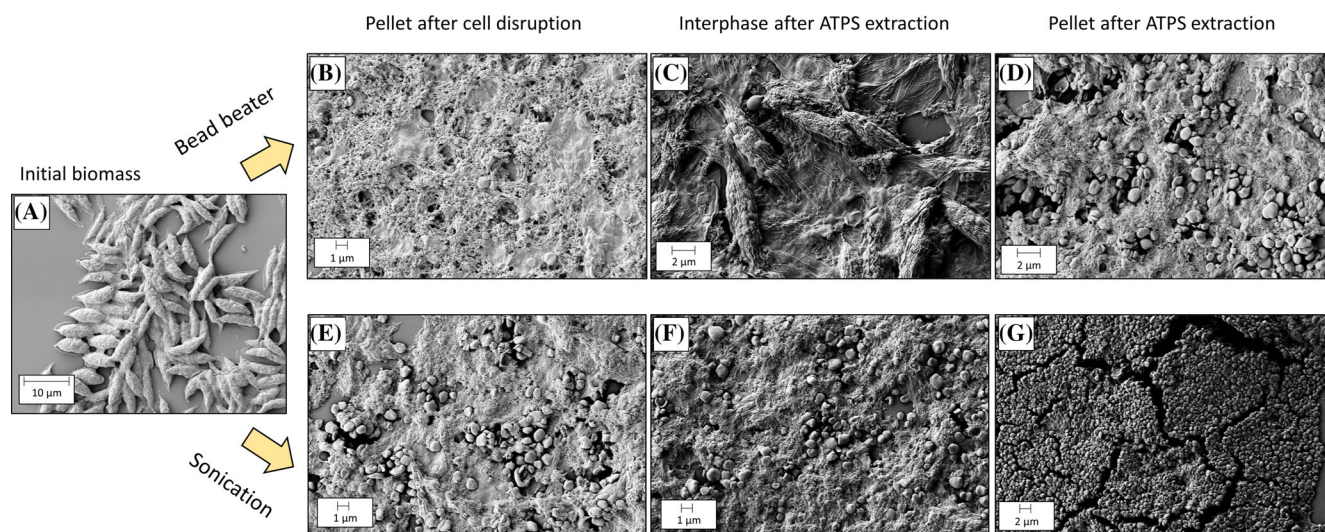


**Figure 4.** SEM images of initial biomass (A); pellet obtained after cell disruption with bead beater (B) and sonication (E); interphase after the third cycle of ATPS extraction on disrupted biomass from bead beater (C) and sonication (F); pellet phase after the third cycle of ATPS extraction on disrupted biomass from bead beater (D) and sonication (G).

present study of ChCl instead of ChDhp, and by the different microalgal species (*N. oleoabundans*) used by Suarez Ruiz *et al.*, which has a different biochemical composition. The biomass used in this study contained indeed a higher initial starch content (33%) as compared to the biomass used by Suarez Ruiz *et al.* (14%). In addition, there are significant differences between the cell walls of *T. obliquus* and *N. oleoabundans*. The latter microalga presents a cell wall mainly composed of proteins (31.5%), lipids (22%) and carbohydrates (24%),<sup>29</sup> while *Scenedesmus* cell wall contains a higher amount of carbohydrates (40%) and less proteins (15%).<sup>23</sup> Finally, preliminary data indicate that *N. oleoabundans* starch is smaller than *T. obliquus* starch (Table 1), which could induce a lower settleability in the bottom pellet.

The morphologies of the interphases obtained after 3 ATPS cycles looked different starting from the biomass lysates produced by bead milling and sonication. In the case of sonication, the interphase in ATPS (Fig. 4(F)) was quite similar to the initial lysate biomass (Fig. 4(E)). When applying bead milling, the interphase obtained at the end of the extraction was rich in empty cell walls (Fig. 4(C)), that appeared as thin sheets. These sheets were also found in suspension in the water-ChCl phase. The pellet phase recovered at the bottom of the water-ChCl phase was also different between bead milling and sonication. The pellets obtained after sonication appeared much more enriched in starch granules (Fig. 4(E)–(G)) as compared to the pellets after cell disruption operated with bead milling (Fig. 4(B)–(D)). For all, a visible

fraction of residual biomass was still visible surrounding the starch granules. In the pellet after sonication and ATPS (Fig. 4(G)), there were large areas completely made of starch granules, and some other areas showing both starch granules and residual biomass in equivalent proportions. The purity of starch in the pellet phase recovered after sonication and ATPS (3 cycles) was equal to  $50 \pm 5\%$  as dry weight. This remained substantially equal independent of the ATPS treatment because this percentage was the same in the pellet recovered after sonication and in those recovered after 1 cycle or 3 cycles of ATPS. This was probably due to a comparable solubilization of water-soluble compounds (proteins) in water and in ChCl-water solution, while the pigments removed by the PPG 400 phase did not contribute remarkably on changing the purity of the starch.

Although sonication gave better starch separation than bead milling, it should be underlined that the sonication probe was affected by relevant superficial erosion during the treatment (Supporting Information, Fig. S4), which resulted in the release of metal fragments inside the sample. This phenomenon is quite common for sonication and was described in previous studies.<sup>30,31</sup> The released metal fragments inevitable contaminated the recovered pellet, which resulted light grey. This release was measured making a sonication test with only water and separating the released metal fragments with 0.7 µm filter. These fragments were 11 mg in 20 mL, after 3 h of treatment, corresponding to  $\sim 3\%$  of the starch mass in the pellet. This negative effect could be overcome by using an extraction chamber not in direct contact with the probe; however, this would inevitably reduce sonication yield and cell disruption rate.

The ChCl phase was analyzed for its glucose content because microalgae contain a certain fraction of it that was expected to be extracted mainly in the more polar phase.<sup>10</sup> In this phase, the glucose concentration was the same independently of the cell disruption method used, and corresponded to  $10.5\% \pm 1.5\%$  of the initial microalgal biomass.

#### ATPS extraction of pigments

The microalgal biomass contained a relevant number of pigments that were extracted in the PPG400 phase with the ATPS (Fig. 5). The microalgal biomass was characterized for the initial content

**Table 1.** Comparison among mean starch granule size (diameter) found in this study and in previous studies

Species	Mean size (µm)		Reference
	(n° analyzed granules)		
<i>Chlorella sorokiniana</i>	0.96–1.27 (n. d.)		7
<i>Neochloris oleoabundans</i>	0.52 (7)		35
<i>Chlorella sorokiniana</i>	1.5 (n. d.)		1
<i>Tetradismus obliquus</i>	0.93 (100)		This study

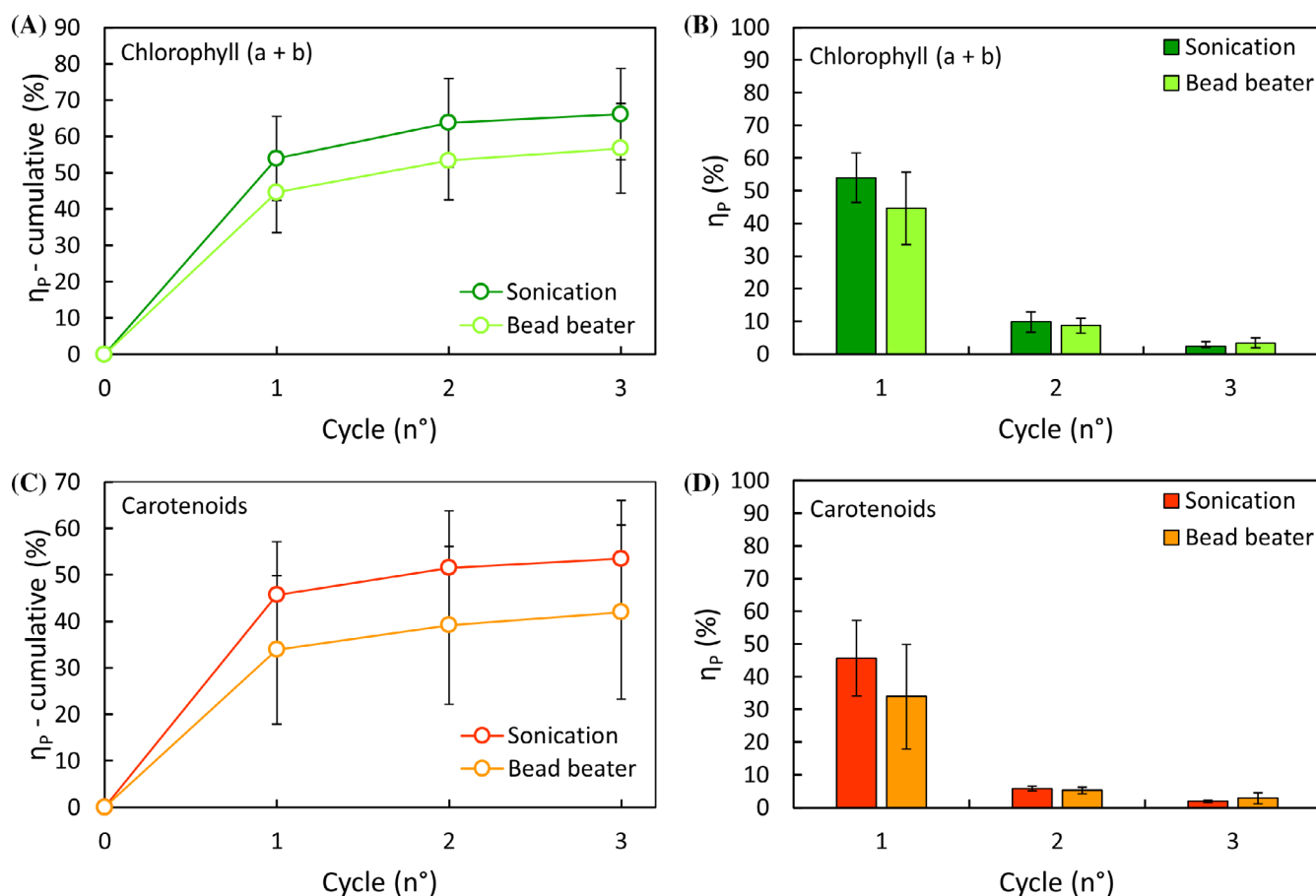


**Figure 5.** Chlorophyll and carotenoid recovery yield (%) calculated as cumulative yield (A and C respectively) and for each single extraction cycle (B and D respectively). Mean value  $\pm$  SE,  $n = 3$ .

of pigments before being treated with sonication and bead milling. The biomass contained  $1.9\% \pm 0.4\%$  of pigments, 55% of which was chlorophyll a, 26% chlorophyll b, and 19% carotenoids. Up to 57–66% Chlorophylls (a + b) and up to 42–53% carotenoids were recovered after three ATPS extraction cycles. There was no significant difference given by the two pre-treatment methods used for cell disruption. Some residual pigments remained in the pellet phases, which remained still green at the end of the extraction with ATPS (Supporting Information, Fig. S3), for both treatments. The ChCl phase and the interphase were colorless at the end of the extraction, for both the pre-treatments, indicating a negligible content of residual pigments. The pigment extraction yield was lower than the 98% yield attained for lutein from *N. oleoabundans* by using PPG400- ChDhp.<sup>11</sup> As for the starch, also for the pigments these relevant differences could be determined by the different microalgal species used. For instance, while the *N. oleoabundans* used by Suarez Ruiz *et al.* contained mainly lutein as pigment, in the biomass used here in this study 81% of the pigments was made of Chlorophylls (a + b), that have lower polarity and are often linked to proteins in the chloroplast membranes. The fact that both chlorophylls and carotenoids were not completely extracted can be an indication that a fraction of these pigments was still linked to biomass residues. Yet, the pigment extraction yield was calculated with respect to their initial amount inside the biomass before cell disruption (Eqn (9)). Therefore, any loss occurred during the cell disruption treatment was included in the yield in this study. When only the extracted

pigments were considered, it was found that almost all pigments were extracted in the first ATPS cycle (Fig. 5(B)–(D)), these were  $81\% \pm 1\%$  for chlorophylls (a + b) and  $83\% \pm 3\%$  for carotenoids, without difference for the cell disruption method. This means that an optimized process could be carried out with only one extraction cycle, reducing substantially the consumption of solvent and energy cost, which increase with the number of extraction cycles performed.<sup>32</sup>

#### Assessment of energetic yield of the extraction with sonication

The sonication treatment gave the better results in term of biomolecule separation. However, to evaluate the potential of industrial scale-up, energy consumption of this technology must be also assessed. In this respect, insufficient information was found in literature about energy consumption of sonication treatment applied to the microalgal cell disruption. Therefore, the performance of the sonication treatment was evaluated more in depth by assessing the energy demand of this cell disruption process. A constant 150 W power (P) was applied during the  $T_{on}$  periods and thus the consumed energy (E) could be calculated by Eqn (10):

$$E = PT_{on} \quad (10)$$

Based on Eqn (10) and the kinetic equation for cell disruption (Eqn (3)), the specific energy demand ( $\eta_E$ ) for disrupted cells was then calculated as follows:



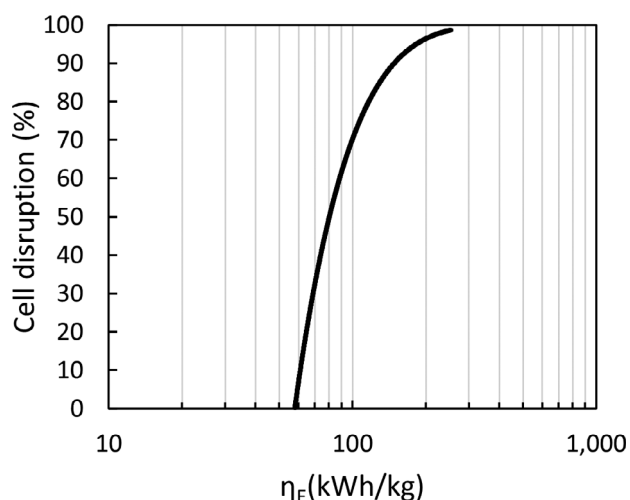


**Figure 6.** Energy demand of the cell disruption treatment carried out with sonication. The energy demand is expressed as kWh of consumed energy per kg of disrupted cells. Data were calculated by Eqn (11) for  $90 \text{ g L}^{-1}$  initial biomass concentration.

$$\eta_E = \frac{PT_{on}}{V(C_{0,cell} - C_{cell}(T_{on}))} = \frac{PT_{on}}{V(C_{0,cell}(1 - e^{-kT_{on}}))} \quad (11)$$

with  $V$  denoting the volume of the sonication chamber. The results of Eqn (11) are reported in Fig. 6. During the first part of the treatment, the energy demand for disrupted cells increases slightly, varying from  $50 \text{ kWh kg}^{-1}$  to  $100 \text{ kWh kg}^{-1}$  to disrupt from 0.2% to 62% cells ( $t = \tau$ ), while further  $82 \text{ kWh kg}^{-1}$  were required to increase the cell disruption yield from 62% to 95% ( $3\tau$ ). This energy consumption is likely still too high for starch utilization in low-cost applications, as bioplastics, but it could be acceptable for high value applications as for instance food additive, pharmaceutical or medical applications (e.g. antimicrobial materials). The energy demand is higher than those reported in other studies for other cell disruption methods (usually between  $0.3\text{--}10 \text{ kWh kg}^{-1}$ ).<sup>13</sup> However, in these previous studies the energy demand was usually calculated for undefined cell disruption yields, for different microalgal species and often calculated at arbitrary extraction yield of solvent soluble biomolecules, as soluble proteins, for which a complete cell disruption is not required.<sup>21</sup>

A general scheme of the possible industrial process is proposed in Fig. 7. This process scheme includes a single ATPS cycle, by which large part of starch and extractable pigments could be

separated. The process includes a three-phase centrifugation to separate the pellet phase, the PPG400 phase and the ChCl phase with a single step. The regeneration of the solvents is an open issue that is worth of investigation in future studies. The ChCl phase could be recovered by ultrafiltration, while the PPG400 phase by back extraction of pigments in a hydrophobic solvent immiscible in water (e.g. hexane).

### Properties of the microalgal starch

The physical–chemical properties of the starch can strongly influence the efficiency of the extraction and separation processes. The radius ( $r$ ) of the granules influences the settling velocity ( $v$ ) inside a fluid (liquid phase) during sedimentation or centrifugation ( $v \propto r^2$  according to the Stoke's Law). The distribution of *T. obliquus* starch granule size was measured in this study (Fig. 8). The distribution of the diameter was well described by a Gaussian's function (Fig. 8(A)), with  $0.93 \mu\text{m}$  mean value and  $\pm 0.14 \mu\text{m}$  SD. The size distribution of granules was very narrow, with 95% of granules between  $0.645\text{--}1.215 \mu\text{m}$ . For comparison, superior plants like corn, barley, and wheat usually have bimodal distributions (A-type and B-type starch) with sizes of  $1\text{--}5 \mu\text{m}$  (B-type) and  $10\text{--}36 \mu\text{m}$  (A-type).<sup>6,33</sup> The A-type is predominant in superior plants and the resulting average size of starch granules is about one order of magnitude higher as compared to microalgal starch.<sup>34</sup> The size distribution found here in this study is even more narrow than that previously reported for the microalga *Chlorella sorokiniana*, which was  $0.8\text{--}5.3 \mu\text{m}$  with 15% particles  $>5.3 \mu\text{m}$ .<sup>1</sup> However, in this previous study the distribution was analyzed by a laser granulometer, therefore any foreign particle, as residual cell fragments, could give interferences. Instead in this study the image analysis allowed to include selectively only the starch granules.

The difference in granule size can contribute to explain the different behavior between corn starch and *N. oleoabundans* starch, which was observed in the ATPS by Suarez Ruiz *et al.*<sup>10</sup> A difference in starch granule size might also explain the different behaviors observed for *N. oleoabundans* and *T. obliquus* starch in ATPS. Since *N. oleoabundans* starch granules have mean size ( $0.52 \mu\text{m}$ ) about half as compared to *T. obliquus* starch (Table 1), they will have a settling velocity 4 times lower than *T. obliquus* starch. For sake of clarity, it should be underlined that we calculated the average starch granule size for *N. oleoabundans* from a single image, reported by Giovanardi *et al.*,<sup>35</sup> that only included seven granules. The mean starch granule size of *T. obliquus* was close to that found for *C. sorokiniana*, which was a little larger (Table 1).

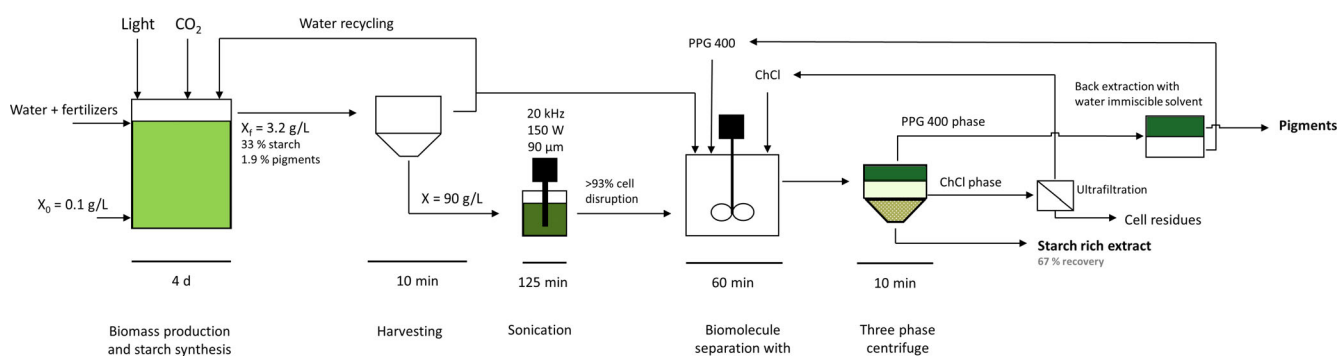


**Figure 7.** Summary of the process scheme developed in this study to produce and extract starch and pigments from microalgae. The scheme also includes two possible ways to regenerate the ChCl and PPG400 phase by using ultrafiltration and back extraction with solvent, respectively.

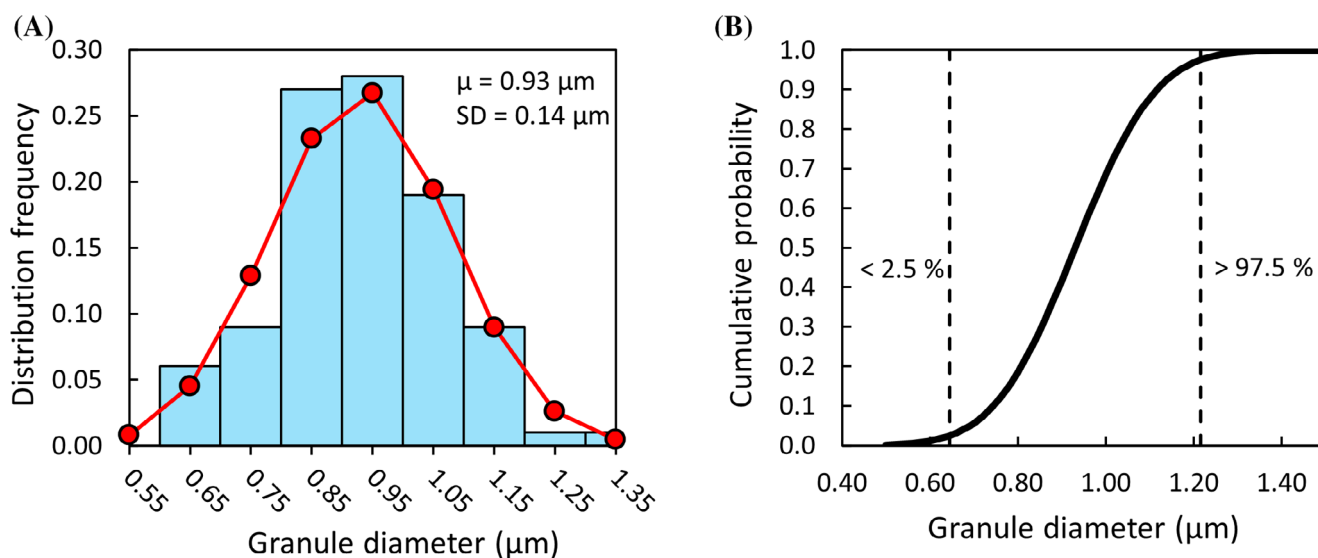


**Figure 8.** Starch granule size distribution measured on starch sample obtained in the pellet phase after ATPS extraction from biomass obtained after sonication treatment. (A) Distribution frequency obtained for 9 bins (0.1 μm each one) with experimental data (histograms) and Gaussian distribution (circles) with  $\mu = 0.93$  and  $\sigma = 0.14$ . (B) Cumulative probability obtained for Gaussian distribution with  $\mu = 0.93$  and  $\sigma = 0.14$ . The diameter was measured on 100 starch granules.

Qualitatively, the starch granules observed with SEM showed two different morphologies (Fig. 4). The large part of the granules showed a globular-shape, which is characteristic of stroma starch, while a little part of granules showed a cup-shape, which is characteristic of pyrenoids starch. These two morphologies are typical for microalgal starch and were described also for *C. sorokiniana* and *N. oleoabundans*.<sup>7,12,35</sup>

An important physical property of starch is the temperature at which gelatinization occurs. This value determines the temperature to which a water-starch suspension should be heated to attain starch gelatinization, which includes a phase transition from the native crystalline form to a soluble amorphous gel. This phase transition is needed to ensure starch processability in practical applications as for producing bioplastics or food cooking. The gelatinization of starch is usually described by three specific temperatures: onset temperature (temperature at which the gelatinization starts), peak temperature (peak in viscosity variation) and completion temperature (ending of the process). The gelatinization temperature was evaluated by observing the starch morphology with optical microscopy. Particularly, a starch-water suspension (using the pellet obtained after sonication and ATPS) was analyzed after heating at different temperature ranges

(Fig. 9). Starch granules remained visible and unchanged in the samples treated up to 35 °C, start to disappear at temperatures of 45–50 °C and eventually disappeared completely when temperatures between 50–55 °C were attained. No crystallization was observed in the sample subsequently cooled down. This behavior was due to the solubilization of starch granules in the form of a gel and was often reported for starch from superior plants.<sup>36</sup> From these results it was deduced that the gelatinization started at temperature between 45–50 °C and was complete at 50–55 °C. To confirm the effective formation of a stable gel, the sample was heated at 55 °C, subsequently cooled down at room temperature and finally observed with SEM. The SEM analyses showed the presence of a uniform gel layer (Fig. 9(E)), significantly different from the granules in the original sample before heating (Fig. 4(G)). These temperature values for starch gelatinization are remarkably lower than the gelatinization temperatures usually found for the starch produced from conventional sources, as corn, potatoes and wheat. For these latter sources, starch gelatinization usually starts at temperatures between 58–71 °C and ends at temperatures between 70–90 °C.<sup>34</sup> The starch gelatinization temperature was reported to be mainly affected by the amylose/amylopectin ratio.<sup>34</sup> However, different previous studies reported

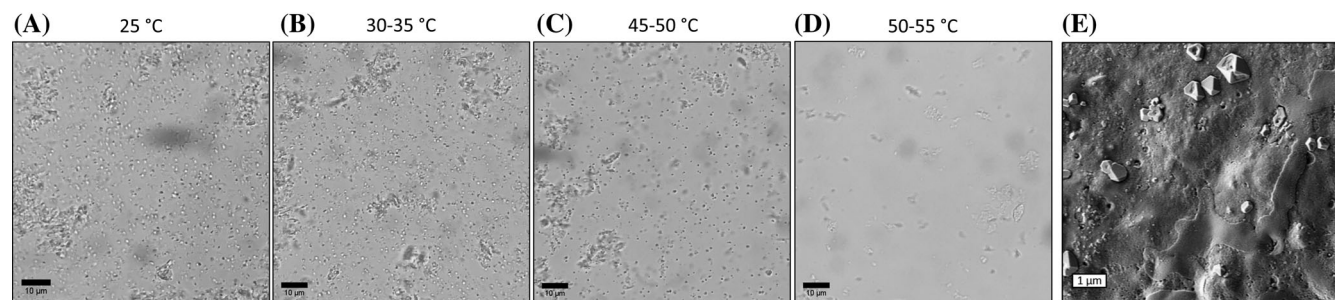


**Figure 9.** Observation with optical microscopy of starch granules treated at different temperatures from 25 °C (A) to 50–55 °C (D). (E) SEM image of gelatinized starch sample after treatment at 55 °C. The analysis was conducted on the pellet phase obtained after ATPS extraction from biomass obtained after sonication treatment.

amylose content in microalgal starch between 17–29%,<sup>1,7</sup> comparable with the starch from conventional plant sources as corn, wheat and potatoes.<sup>34</sup> Probably, factors as granule size and amylopectin chain length are responsible for such difference and deserve therefore to be investigated in future studies. It should be here remarked that the lower gelatinization temperature of microalgal starch introduces significant advantages as compared to conventional starch sources. In addition to reducing the energy consumption required to enforce starch processability in industrial applications, it could also be an advantage for starch-based bioplastic functionalization with bioactive molecules, which are usually thermolabile. The temperature here reported also indicates that every protocol to extract native starch from microalgae should avoid temperature higher than 45 °C.

## CONCLUSIONS

The work described a biorefinery route to produce microalgal starch. Cell disruption kinetics was satisfactorily described by a first order model for sonication and bead milling, with the latter presenting a disruption rate 2.6 times faster. There was a remarkable difference in starch recovery from samples in which a comparable cell disruption yield was achieved with different methods. Indeed, the starch was separated better with ATPS from the biomass lysed by sonication than by bead milling, despite the comparable fraction of disrupted cells. After the sonication, 67% starch was recovered in the residual pellet after ATPS, while after bead milling this was only 40% and remained equally distributed between residual pellet and water-ChCl liquid phase. This insight indicates that the cell disruption yield alone does not allow to predict the recovery yield of starch.

The erosion of the probe tip during sonication released metal particles that contaminated the obtained starch. Pigment extraction occurred mainly in the first extraction cycle (80%) in the PPG 400 phase and was comparable for the two cell disruption methods.

As compared to conventional starch sources, the microalgal starch showed lower gelatinization temperature, between 45–55 °C, and lower mean granule size, with a narrow and normal distribution with  $0.93 \pm 0.14 \mu\text{m}$  diameter. These differences from conventional starch sources can introduce significant advantages in the application of microalgal starch for bioplastic production, including reduced energy consumption and easier functionalization with thermolabile bioactive molecules.

## SUPPORTING INFORMATION

Supporting information may be found in the online version of this article.

## REFERENCE

- Gifuni I, Olivieri G, Krauss IR, D'Errico G, Pollio A and Marzocchella A, Microalgae as new sources of starch: isolation and characterization of microalgal starch granules. *Chem Eng Trans* **57**:1423–1428 (2017).
- Gifuni I, Olivieri G, Pollio A, Franco TT and Marzocchella A, Autotrophic starch production by *Chlamydomonas* species. *J Appl Phycol* **29**:105–114 (2017).
- Breuer G, de Jaeger L, Artus VG, Martens DE, Springer J, Draaisma RB *et al.*, Superior triacylglycerol (TAG) accumulation in starchless mutants of *Scenedesmus obliquus*: (II) evaluation of TAG yield and productivity in controlled photobioreactors. *Biotechnol Biofuels* **7**:70 (2014).
- Ran W, Xiang Q, Pan Y, Xie T, Zhang Y and Yao C, Enhancing photosynthetic starch production by  $\gamma$ -aminobutyric acid addition in a marine green microalga *Tetraselmis subcordiformis* under nitrogen stress. *Ind Eng Chem Res* **59**:17103–17112 (2020).
- Lutz G, Ciurlu A, Chiellini C, Di Caprio F, Concas A and Dunford NT, Latest developments in wastewater treatment and biopolymer production by microalgae. *J Environ Chem Eng* **9**:104926 (2021).
- Lindeboom N, Chang PR and Tyler RT, Analytical, biochemical and physicochemical aspects of starch granule size, with emphasis on small granule starches: a review. *Starch-Stärke* **56**:89–99 (2004).
- Tanadul O, Vanderghenst JS, Beckles DM, Powell ALT and Labavitch JM, The impact of elevated CO<sub>2</sub> concentration on the quality of algal starch as a potential biofuel feedstock. *Biotechnol Bioeng* **111**:1323–1331 (2014).
- Alhattab M, Kermanshahi-pour A and Brooks MS, Microalgae disruption techniques for product recovery: influence of cell wall composition. *J Appl Phycol* **1**:61–88 (2019).
- Delrue B, Fontaine T, Routier F, Decq A, Wieruszkeski JM, Van Den Koornhuysen N *et al.*, Waxy *Chlamydomonas reinhardtii*: monocellular algal mutants defective in amylose biosynthesis and granule-bound starch synthase activity accumulate a structurally modified amylopectin. *J Bacteriol* **174**:3612–3620 (1992).
- Suarez Ruiz CA, Baca SZ, van den Broek LA, van den Berg C, Wijffels RH *et al.*, Selective fractionation of free glucose and starch from microalgae using aqueous two-phase systems. *Algal Res* **46**:101801 (2020).
- Suarez Ruiz CA, Kwaijtaal J, Peinado OC, Van Den Berg C, Wijffels RH *et al.*, Multistep fractionation of microalgal biomolecules using selective aqueous two-phase systems. *ACS Sustain Chem Eng* **8**:2441–2452 (2020).
- Izumo A, Fujiwara S, Oyama Y, Satoh A, Fujita N, Nakamura Y *et al.*, Physicochemical properties of starch in *Chlorella* change depending on the CO<sub>2</sub> concentration during growth: comparison of structure and properties of pyrenoid and stroma starch. *Plant Sci* **117**:1138–1147 (2007).
- Nitsos C, Filali R, Taidi B and Lemaire J, Current and novel approaches to downstream processing of microalgae: a review. *Biotechnol Adv* **45**:107650 (2020).
- Di Caprio F, Altamari P, Iaquaniello G, Toro L and Pagnanelli F, *T. obliquus* mixotrophic cultivation in treated and untreated olive mill wastewater. *Chem Eng Trans* **64**:625–630 (2018).
- de Jaeger L, Verbeek RE, Draaisma RB, Martens DE, Springer J, Eggink G *et al.*, Superior triacylglycerol (TAG) accumulation in starchless mutants of *Scenedesmus obliquus*: (I) mutant generation and characterization. *Biotechnol Biofuels* **7**:69 (2014).
- Lichtenthaler HK, [34] Chlorophylls and carotenoids: pigments of photosynthetic biomembranes. *Methods Enzymol* **148**:350–382 (1987).
- Breuer G, Lamers PP, Martens DE, Draaisma RB and Wijffels RH, Effect of light intensity, pH, and temperature on triacylglycerol (TAG) accumulation induced by nitrogen starvation in *Scenedesmus obliquus*. *Bioresour Technol* **143**:1–9 (2013).
- Breuer G, Martens DE, Draaisma RB, Wijffels RH and Lamers PP, Photosynthetic efficiency and carbon partitioning in nitrogen-starved *Scenedesmus obliquus*. *Algal Res* **9**:254–262 (2015).
- Halim R, Rupasinghe TWT, Tull DL and Webley PA, Mechanical cell disruption for lipid extraction from microalgal biomass. *Bioresour Technol* **140**:53–63 (2013).
- Postma PR, Suarez-Garcia E, Safi C, Yonathan K, Olivieri G, Barbosa MJ *et al.*, Energy efficient bead milling of microalgae: effect of bead size on disintegration and release of proteins and carbohydrates. *Bioresour Technol* **224**:670–679 (2017).
- Safi C, Rodriguez LC, Mulder WJ, Engelen-Smit N, Spekking W, Van den Broek LA *et al.*, Energy consumption and water-soluble protein release by cell wall disruption of *Nannochloropsis gaditana*. *Bioresour Technol* **239**:204–210 (2017).
- Taleb A, Kandilian R, Touchard R, Montalescot V, Rinaldi T, Taha S *et al.*, Screening of freshwater and seawater microalgae strains in fully controlled photobioreactors for biodiesel production. *Bioresour Technol* **218**:480–490 (2016).
- Baudelet PH, Ricochon G, Linder M and Muniglia L, A new insight into cell walls of Chlorophyta. *Algal Res* **25**:333–371 (2017).
- Patel S and Kannan DC, A method of wet algal lipid recovery for biofuel production. *Algal Res* **55**:102237 (2021).
- Halim R, Harun R, Danquah MK and Webley PA, Microalgal cell disruption for biofuel development. *Appl Energy* **91**:116–121 (2012).

- 26 Safi C, Ursu AV, Laroche C, Zebib B, Merah O, Pontalier PY *et al.*, Aqueous extraction of proteins from microalgae: effect of different cell disruption methods. *Algal Res* **3**:61–65 (2014).
- 27 Suarez Ruiz CA, Emmery DP, Wijffels RH, Eppink MHM and van den Berg C, Selective and mild fractionation of microalgal proteins and pigments using aqueous two-phase systems. *J Chem Technol Biotechnol* **93**:2774–2783 (2018).
- 28 Shaukat S and Buchner R, Densities, viscosities [from (278.15 to 318.15) K], and electrical conductivities (at 298.15 K) of aqueous solutions of choline chloride and chloro-choline chloride. *J Chem Eng Data* **56**:4944–4949 (2011).
- 29 Rashidi B and Trindade LM, Detailed biochemical and morphologic characteristics of the green microalga *Neochloris oleoabundans* cell wall. *Algal Res* **35**:152–159 (2018).
- 30 Mawson R, Rout M, Ripoll G, Swiergon P, Singh T, Knoerzer K *et al.*, Production of particulates from transducer erosion: implications on food safety. *Ultrason Sonochem* **21**:2122–2130 (2014).
- 31 Betts JN, Johnson MG, Rygiewicz PT, King GA and Andersen CP, Potential for metal contamination by direct sonication of nanoparticle suspensions. *Environ Toxicol Chem* **32**:889–893 (2013).
- 32 Di Caprio F, Altimari P and Pagnanelli F, Sequential extraction of lutein and  $\beta$ -carotene from wet microalgae biomass. *J Chem Technol Biotechnol* **95**:3024–3033 (2020).
- 33 Buléon A, Colonna P, Planchot V and Ball S, Starch granules: structure and biosynthesis. *Int J Biol Macromol* **23**:85–112 (1998).
- 34 Thakur R, Pristijono P, Scarlett CJ, Bowyer M, Singh SP and Vuong QV, Starch-based films: major factors affecting their properties. *Int J Biol Macromol* **132**:1079–1089 (2019).
- 35 Giovanardi M, Ferroni L, Baldisserotto C, Tedeschi P, Maietti A, Pantaleoni L *et al.*, Morphophysiological analyses of *Neochloris oleoabundans* (Chlorophyta) grown mixotrophically in a carbon-rich waste product. *Protoplasma* **250**:161–174 (2013).
- 36 Błaszczak W and Lewandowicz G, Light microscopy as a tool to evaluate the functionality of starch in food. *Foods* **9**:670 (2020).